Sciencexpress Reports

Molecular Gas Clumps from the Destruction of Icy Bodies in the β Pictoris Debris Disk

W. R. F. Dent,[1]* M. C. Wyatt,[2] A. Roberge,[3] J.-C. Augereau,[4] S. Casassus,[5] S. Corder,[1] J. S. Greaves,[6] I. de Gregorio-Monsalvo,[1,7] A. Hales,[1] A. P. Jackson,[2,8] A. Meredith Hughes,[9] A.-M. Lagrange,[4] B. Matthews,[10] D. Wilner[11]

[1]ALMA Santiago Central Offices, Alonso de Córdova 3107, Vitacura, Casilla 763 0355, Santiago, Chile. [2]Institute of Astronomy, Madingley Road, Cambridge CB3 0HA, UK. [3]Exoplanets and Stellar Astrophysics Lab, NASA Goddard Space Flight Center, Greenbelt, MD 20771, USA. [4]UJF-Grenoble 1/CNRS-INSU, Institut de Planétologie et d'Astrophysique de Grenoble (IPAG), UMR 5274, Grenoble, F-38041, France. [5]Departamento de Astronomía, Universidad de Chile, Casilla 36-D, Santiago, Chile. [6]Dept. of Astronomy, University of St. Andrews, North Haugh, St. Andrews, UK. [7]European Southern Observatory, Karl-Schwarzschild Str. 2, 85748, Garching, Germany. [8]School of Earth and Space Exploration, Arizona State University, ISTB4, 781 E Terrace Rd., Tempe, AZ 85287–6004, USA. [9]Wesleyan University Department of Astronomy, Van Vleck Observatory, 96 Foss Hill Drive, Middletown, CT 06459, USA. [10]National Research Council of Canada, Herzberg Astronomy & Astrophysics Programs, 5701 West Saanich Road, Victoria, BC, Canada, V9E 2E7, and Department of Physics & Astronomy, University of Victoria, Finnerty Road, Victoria, BC, V8P 5C2, Canada. [11]Smithsonian Astrophysical Observatory, 60 Garden St., MS 42, Cambridge, MA 02138, USA.

*Corresponding author. E-mail: wdent@alma.cl

Many stars are surrounded by disks of dusty debris formed in the collisions of asteroids, comets and dwarf planets. But is gas also released in such events? Observations at sub-mm wavelengths of the archetypal debris disk around β Pictoris show that 0.3% of a Moon mass of carbon monoxide orbits in its debris belt. The gas distribution is highly asymmetric, with 30% found in a single clump 85 AU from the star, in a plane closely aligned with the orbit of the inner planet, β Pic b. This gas clump delineates a region of enhanced collisions, either from a mean motion resonance with an unseen giant planet, or from the remnants of a collision of Mars-mass planets.

Debris disks are the end product of collisional cascades of km-sized bodies orbiting stars (including the Sun), and are normally thought to contain negligible gas. At a distance of 19.44 parsec (*1*) and age of 20 million years (*2*), β Pictoris is one of the closest, brightest and youngest examples. Its edge-on disk was the first to be imaged in scattered light, showing the distribution of micron-sized dust grains (*3*). Various subsequent observations have provided evidence of infalling comets within a few Astronomical Units (AU) of the star (*4*), a massive planet at ~10 AU (*5*), as well as atomic gas extending out to ~300 AU (*6*); it is still unclear how these features are linked. By observing such debris disks at mm wavelengths, it is possible to trace the mm-sized dust and, by inference, the parent bodies of the collisional cascade, known as planetesimals (*7*).

We observed β Pic using the Atacama Large Millimeter/submillimeter Array (ALMA) at a wavelength of 870 μm in both the continuum and the J = 3-2 ^{12}CO line with a resolution of 12AU (*8*). The continuum image (Fig. 1A) shows maxima in the surface brightness ~60 AU either side of the star. At separations from 30-80 AU the continuum is, on average, 15% brighter to the southwest. These results indicate that the mm grains lie in a broad slightly asymmetric belt nearly co-located with the disk of sub-micron reflecting dust (*9*). The total flux of 60 ± 6 mJy corresponds to a dust mass of $4.7 \pm 0.5 \times 10^{23}$ kg ($6.4 M_{Moon}$), if we assume a standard dust mass opacity (0.15 m^2 kg^{-1} at 850 μm) and temperature of 85 K (*10*).

The planet β Pic b was close to maximum SW elongation at the time of the observations, with a projected separation of 8.7 AU (*11*). Its location is coincident with a dip in the continuum surface brightness at a significance level of 4σ, suggesting that it may influence the innermost dust distribution.

ALMA also detected the disk in the ^{12}CO J = 3-2 transition (Fig. 1B), with a clear velocity gradient along the major axis, illustrated in the position-velocity (PV) diagram (Fig. 2). This shows the characteristic distribution of a broad belt of orbiting gas, with inner and outer radii of 50 and 160 AU, and a peak around 85 AU. No gas emission is seen inside 50 AU. The CO distribution is, on average, a factor of 2 brighter to the southwest, and a similar asymmetry was seen in the mid-infrared emission (*12*). Unlike the sub-mm continuum, the CO clump is offset by ~5 AU above the main disk plane (Fig. 1B) and is more closely aligned with the inner planet b Pic b and a secondary disk seen in scattered light (*5*, *9*).

The CO J = 3-2 emission totals $7.6 \pm 0.8 \times 10^{-20}$ W/m^2. Assuming a range of possible excitation temperatures from 20 K [measured from UV absorption lines (*13*)], to 85 K [the dust equilibrium temperature (*10*)], this corresponds to a CO mass of 1.7×10^{20} kg ($0.0023 M_{Moon}$) within a factor of 2. Toward the star itself, the total CO column is $2.5_{(+2.5,-1.2)} \times 10^{15}$ cm^{-2} ; results from UV absorption line measurements range between 0.6-2.1 × 10^{15} cm^{-2} (*13*), indicating that at least 10% of the CO along this line-of-sight lies in front of the star.

The attenuation through the disk due to dust or CO self-shielding is low and, at radii >50 AU, CO is destroyed mostly by UV photons from the ambient interstellar medium (ISM) (*14*). The CO photodissociation timescale in the unshielded outer disk will be ~120 yrs (*15*) - substantially less than the 600-year orbital period at 85 AU. Unless we are observing β Pic at a very unusual time (i.e., ≤100 years after a collision) then the CO must be continuously replenished, with a steady-state production rate of $\sim 1.4 \times 10^{18}$ kg/yr. The source of CO is likely the icy debris (grains, comets and planetesimals) in the disk (*16*). In our own solar system, comets are mostly composed of refractory silicate grains together with H_2O and CO ices, with a typical CO/H_2O ratio of 0.01-0.1 (*17*). Although CO sublimates at ~20K - substantially less than the 85 K dust temperature in the β Pic disk - it can be trapped in H_2O ice at temperatures up to ~140 K (*18*), which could occur in radiative equilibrium as close as 30 AU from β Pic (*14*). At larger distances, photodesorption or collisions can release this CO into the gas phase. Photodesorption (a.k.a. UV sputtering) of mm-sized ice grains (*19*) in a dust clump with 10% of the total disk mass would produce CO at a rate that is ~10 times lower than our observations show. The CO linewidth measured directly toward the star is ~1 km/s (Fig. 2), suggesting the velocity dispersion is lower than the 6km/s thought necessary for collisions to directly vaporize ice (*20*). However icy parent bodies being shattered in multiple lower velocity collisions may release much of the entrapped CO as gas, leaving the less volatile H_2O ice behind. To sustain the gas production rate with a CO ice release fraction of 0.1, the required mass loss of colliding grains would be $\sim 1.4 \times 10^{19}$ kg/yr, equivalent to the destruction of a large com-

et every 5 min. If sustained over the lifetime of β Pic, ~50M_{Earth} of icy bodies will have been removed.

Continual replenishment of CO may explain another puzzle. In the absence of a braking mechanism many of the atomic species such as Na found around β Pic should be blown out from the central star under the force of radiation pressure (*21*–*23*). Carbon is overabundant relative to other metals, by factors of 18 to 400 (*21*, *22*), and has been proposed as the mechanism that allows the ionized gas to remain bound to the star. C+ couples to other ions through Coulomb forces; and since it feels weak radiation pressure from the central star, it tends to brake all the gas. The origin of the unusual carbon overabundance may be explained if CO is being rapidly released in the clump, then dissociated and ionized before being spread throughout the disk. In steady state, the relative C+/CO abundance implies that C+ is being removed on a timescale of 3×10^3-10^4 yrs; since this is several orbital timescales at 85 AU, the braking gas can be spread throughout the disk.

If the gas is on circular Keplerian orbits, each point in the PV diagram corresponds to one of two points in the disk. Figure 3 shows possible deprojections of the data to form the face-on gas distribution (*8*). A compact clump of CO is found at 85 AU radius which contains ~30% of the flux, along with an extended "tail" of emission. The radial distribution of the mm dust can also be derived (*8*, *12*), and shows excess around this radius in the southwest (Fig. 3C). The mm dust shows an abrupt drop in density around 130 AU radius, coincident with a change in slope in the radial distribution of scattered light. This was interpreted as a transition from a dust-producing planetesimal belt to a region dominated by submicron-sized grains blown out by radiation pressure (*9*, *24*).

What is the origin of the CO clumps and corresponding mid-infrared and continuum features? There are two possible interpretations, both requiring planet-mass objects in the outer disk, but with different predictions for the deprojected gas distribution. In the first (Fig. 3A), outward migration of a planet traps planetesimals into both the 2:1 and 3:2 mean motion resonances, resulting in a distribution with two clumps of asymmetric brightness on opposite sides of the star that orbit with the planet (*25*). Planetesimal collisions would occur most frequently in the clumps which would then be the most vigorous production sites of both CO and the short-lived micron-sized grains seen in mid-infrared images (*12*). The morphology of the clumps constrains the planet's mass and migration parameters (*25*). Notably the planet must be >10M_{Earth} to have captured material into its 2:1 resonance, and it would currently be close to the inner edge of the gas/dust belt, ~90 degrees in front of the SW clump. The CO clump's "tail" would point in the opposite direction to the rotation, and its' length given by the ratio of CO photodissociation lifetime to the synodic period.

The alternative interpretation (Fig. 3B) is that the CO and micron-sized dust originate in a single recent collision (*12*, *26*). Since the clump also contributes ~10% of the flux in our sub-mm continuum image, the parent body must have ~Mars mass, as giant impacts typically release ~10% of the progenitor's mass as debris (*27*). While collisional debris persists in a clump for ~100 yr after such an event, it is more likely that the collision occurred ~0.5 Myr ago, with the asymmetry arising because the orbits of all collisional debris pass through the collision point, a region which would retain a high density and collision rate (*26*). Such a clump would be stationary, and the CO "tail" would lie in the rotation direction, with a length given by the ratio of photodissociation time to sidereal period (Fig. 3B).

Tentative evidence has been published for the clump's motion (*28*), which if confirmed would favor the resonance interpretation. Either way these observations provide a valuable opportunity to ascertain the prevalence of planet-sized objects at large orbital distances in this disk.

The CO gas detected in β Pic is unusual among debris disks. So far, two others have been detected in CO [49 Cet and HD21997 (*16*)] and one in OI [HD172555 (*29*)]. Most debris disks are presumed to contain icy grains, so we would expect all such systems to host CO and its photodissociation products. The high collision rates found in clumps may substantially enhance the gas abundance. If CO is formed in collisions, its brightness will scale as the collision rate, which is proportional to $v_r n_d^2$, where v_r is the collision velocity and n_d is the number of dust grains. Both n_d and v_r are enhanced in clumps due to resonances and giant impacts, increasing collision rates by factors of up to 10-100 (*7*, *26*). The presence of these clumps can increase the overall collision rate and CO flux from a disk by an order of magnitude. The CO and compact clump in the β Pic disk indicates a period of intense activity, driven by planets or planet collisions.

References and Notes

1. F. van Leeuwen, Validation of the new Hipparcos reduction. *Astron. Astrophys.* **474**, 653–664 (2007). doi:10.1051/0004-6361:20078357
2. A. S. Binks, R. D. Jeffries, A lithium depletion boundary age of 21 Myr for the beta Pictoris moving group. *Mon. Not. R. Astron. Soc.* **438**, L11–L15 (2014). doi:10.1093/mnrasl/slt141
3. B. A. Smith, R. J. Terrile, A circumstellar disk around β Pictoris. *Science* **226**, 1421–1424 (1984). doi:10.1126/science.226.4681.1421
4. A. Vidal-Madjar *et al*., *Astron. Astrophys.* **290**, 245 (1994).
5. A.-M. Lagrange, M. Bonnefoy, G. Chauvin, D. Apai, D. Ehrenreich, A. Boccaletti, D. Gratadour, D. Rouan, D. Mouillet, S. Lacour, M. Kasper, A giant planet imaged in the disk of the young star Pictoris. *Science* **329**, L57 (2010). doi:10.1126/science.1187187
6. A. Brandeker, R. Liseau, G. Olofsson, M. Fridlund, The spatial structure of the β Pictoris gas disk. *Astron. Astrophys.* **413**, 681–691 (2004). doi:10.1051/0004-6361:20034326
7. M. C. Wyatt, Dust in resonant extrasolar Kuiper belts: Grain size and wavelength dependence of disk structure. *Astrophys. J.* **639**, 1153–1165 (2006). doi:10.1086/499487
8. Materials and methods are available as supplementary materials on *Science* Online.
9. D. A. Golimowski, D. R. Ardila, J. E. Krist, M. Clampin, H. C. Ford, G. D. Illingworth, F. Bartko, N. Benítez, J. P. Blakeslee, R. J. Bouwens, L. D. Bradley, T. J. Broadhurst, R. A. Brown, C. J. Burrows, E. S. Cheng, N. J. G. Cross, R. Demarco, P. D. Feldman, M. Franx, T. Goto, C. Gronwall, G. F. Hartig, B. P. Holden, N. L. Homeier, L. Infante, M. J. Jee, R. A. Kimble, M. P. Lesser, A. R. Martel, S. Mei, F. Menanteau, G. R. Meurer, G. K. Miley, V. Motta, M. Postman, P. Rosati, M. Sirianni, W. B. Sparks, H. D. Tran, Z. I. Tsvetanov, R. L. White, W. Zheng, A. W. Zirm, Hubble Space Telescope ACS multiband coronagraphic imaging of the debris disk around β Pictoris. *Astron. J.* **131**, 3109–3130 (2006). doi:10.1086/503801
10. W. R. F. Dent, H. J. Walker, W. S. Holland, J. S. Greaves, Models of the dust structures around Vega-excess stars. *Mon. Not. R. Astron. Soc.* **314**, 702–712 (2000). doi:10.1046/j.1365-8711.2000.03331.x
11. G. Chauvin, A.-M. Lagrange, H. Beust, M. Bonnefoy, A. Boccaletti, D. Apai, F. Allard, D. Ehrenreich, J. H. V. Girard, D. Mouillet, D. Rouan, Orbital characterization of the β Pictoris b giant planet. *Astron. Astrophys.* **542**, A41 (2012). doi:10.1051/0004-6361/201118346
12. C. M. Telesco, R. S. Fisher, M. C. Wyatt, S. F. Dermott, T. J. Kehoe, S. Novotny, N. Mariñas, J. T. Radomski, C. Packham, J. De Buizer, T. L. Hayward, Mid-infrared images of β Pictoris and the possible role of planetesimal collisions in the central disk. *Nature* **433**, 133–136 (2005). Medline doi:10.1038/nature03255
13. A. Roberge, P. D. Feldman, A. M. Lagrange, A. Vidal-Madjar, R. Ferlet, A. Jolly, J. L. Lemaire, F. Rostas, High-resolution Hubble Space Telescope STIS spectra of C I and CO in the β Pictoris circumstellar disk. *Astrophys. J.* **538**, 904–910 (2000). doi:10.1086/309157
14. I. Kamp, F. Bertoldi, *Astron. Astrpophys.* **353**, 276 (2001).
15. R. Visser, E. F. van Dishoeck, J. H. Black, The photodissociation and chemistry of CO isotopologues: Applications to interstellar clouds and circumstellar disks. *Astron. Astrophys.* **503**, 323–343 (2009). doi:10.1051/0004-6361/200912129
16. B. Zuckerman, I. Song, A 40 Myr old gaseous circumstellar disk at 49 Ceti: Massive CO-rich comet clouds at young A-type stars. *Astrophys. J.* **758**, 77 (2012). doi:10.1088/0004-637X/758/2/77
17. K. I. Oberg, A. C. A. Boogert, K. M. Pontoppidan, S. van den Broek, E. F.

van Dishoeck, S. Bottinelli, G. A. Blake, N. J. Evans, The *Spitzer* ice legacy: Ice evolution from cores to protostars. *Astrophys. J.* **740**, 109 (2011). doi:10.1088/0004-637X/740/2/109
18. M. P. Collings, J. W. Dever, H. J. Fraser, M. R. S. McCoustra, D. A. Williams, Carbon monoxide entrapment in interstellar ice analogs. *Astrophys. J.* **583**, 1058–1062 (2003). doi:10.1086/345389
19. A. Grigorieva, Ph. Thebault, P. Artymowicz, A. Brandeker, Survival of icy grains in debris discs. *Astron. Astrophys.* **475**, 755–764 (2007). doi:10.1051/0004-6361:20077686
20. A. G. G. M. Tielens, C. F. McKee, C. G. Seab, D. J. Hollenbach, The physics of grain-grain collisions and gas-grain sputtering in interstellar shocks. *Astrophys. J.* **431**, 321 (1994). doi:10.1086/174488
21. A. Roberge, P. D. Feldman, A. J. Weinberger, M. Deleuil, J.-C. Bouret, Stabilization of the disk around β Pictoris by extremely carbon-rich gas. *Nature* **441**, 724 (2006). doi:10.1038/nature04832
22. J.-W. Xie, A. Brandeker, Y. Wu, On the unusual gas composition in the β Pictoris debris disk. *Astrophys. J.* **762**, 114 (2013). doi:10.1088/0004-637X/762/2/114
23. R. Fernandez, A. Brandeker, Y. Wu, Braking the gas in the β Pictoris disk. *Astrophys. J.* **643**, 509–522 (2006). doi:10.1086/500788
24. J. C. Augereau, R. P. Nelson, A. M. Lagrange, J. C. B. Papaloizou, D. Mouillet, Dynamical modeling of large scale asymmetries in the β Pictoris dust disk. *Astron. Astrophys.* **370**, 447–455 (2001). doi:10.1051/0004-6361:20010199
25. M. C. Wyatt, Resonant trapping of planetesimals by planet migration: Debris disk clumps and Vega's similarity to the solar system. *Astrophys. J.* **598**, 1321–1340 (2003). doi:10.1086/379064
26. A. P. Jackson, M. C. Wyatt, Debris from terrestrial planet formation: The Moon-forming collision. *Mon. Not. R. Astron. Soc.* **425**, 657–679 (2012). doi:10.1111/j.1365-2966.2012.21546.x
27. S. T. Stewart, Z. M. Leinhardt, Collisions between gravity-dominated bodies. II. The diversity of impact outcomes during the end stage of planet formation. *Astrophys. J.* **751**, 32 (2012). doi:10.1088/0004-637X/751/1/32
28. D. Li, C. M. Telesco, C. M. Wright, The mineralogy and structure of the inner debris disk of β Pictoris. *Astrophys. J.* **759**, L81 (2012). doi:10.1088/0004-637X/759/2/81
29. P. Riviere-Marichalar, D. Barrado, J.-C. Augereau, W. F. Thi, A. Roberge, C. Eiroa, B. Montesinos, G. Meeus, C. Howard, G. Sandell, G. Duchêne, W. R. F. Dent, J. Lebreton, I. Mendigutía, N. Huélamo, F. Ménard, C. Pinte, HD 172555: Detection of 63 μm [OI] emission in a debris disc. *Astron. Astrophys.* **546**, L8 (2012). doi:10.1051/0004-6361/201219745

Acknowledgments: This paper makes use of the following ALMA data: ADS/JAO.ALMA#2011.0.00087.S. ALMA is a partnership of ESO (representing its member states), NSF (USA) and NINS (Japan), together with NRC (Canada) and NSC and ASIAA (Taiwan), in cooperation with the Republic of Chile. The Joint ALMA Observatory is operated by ESO, AUI/NRAO and NAOJ. Partial financial support for SC, MCW and AH was provided by Millenium Nucleus P10-022-F (Chilean Ministry of Economy). AR acknowledges support by the Goddard Center for Astrobiology, part of the NASA Astrobiology Institute. MCW was supported by the European Union through ERC grant number 279973, IdG acknowledges support from MICINN (Spain) AYA2011-30228-C03 grant (including FEDER funds), APJ was supported by an STFC postgraduate studentship, and JCA acknowledges the French National Research Agency (ANR) for support through contract ANR-2010 BLAN-0505-01 (EXOZODI).

Supplementary Materials
www.sciencemag.org/cgi/content/full/science.1248726/DC1
Materials and Methods
References

19 November 2013; accepted 20 February 2014
Published online 6 March 2014
10.1126/science.1248726

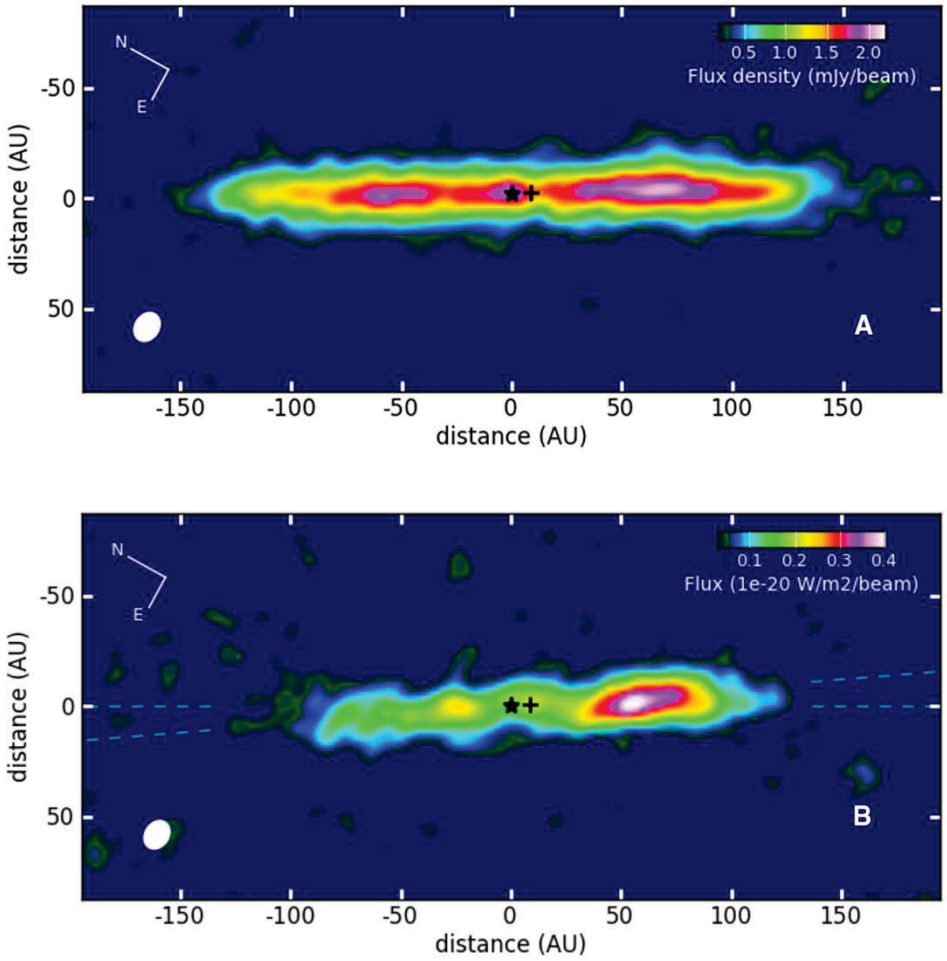

Fig. 1. Images of β Pic using ALMA in continuum and line emission. Both have been rotated by +29 degrees, the position angle of the main dust disk. The beam size (0.56 × 0.71 arcsec) is shown lower left, and the locations of the star and planet on the date of observations are indicated by the asterisk and the cross. (**A**) Continuum emission at 870 μm from the mm dust; the rms noise level is 61 μJy beam^{-1}. (**B**) Total J = 3-2 CO line emission (rest frequency 345.796 GHz); the noise level is 0.02 × 10^{-20} W m^{-2}. The planes of the main and secondary dust disks (*9*) are shown by the dashed lines.

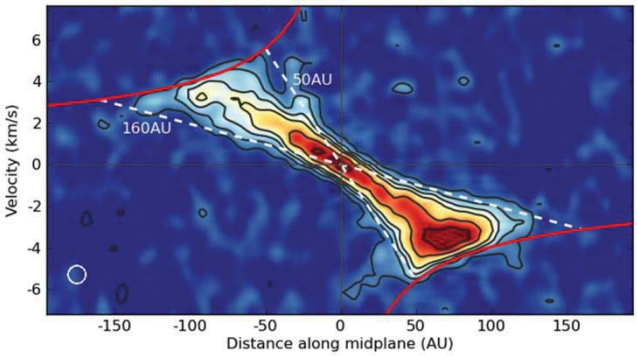

Fig. 2. Velocity distribution along disk major axis. This shows the observed velocity of the CO emission relative to the velocity measured toward the star (which has a centroid of +20.3 ± 0.1 km/s, in the barycentric reference frame). Gas on the brighter SW side is approaching us; the two dashed white lines represent the velocity we would measure from gas at the inner and outer radii of the CO belt. The solid red lines show the true orbital velocity, the maximum observed velocity from gas at the tangential point, as a function of distance from the star, assuming a stellar mass of $1.75M_{solar}$. Contours are 10, 20, 30, 40, 60, 80% of the peak (0.06 Jy/beam). The spectral/spatial resolution is illustrated lower left.

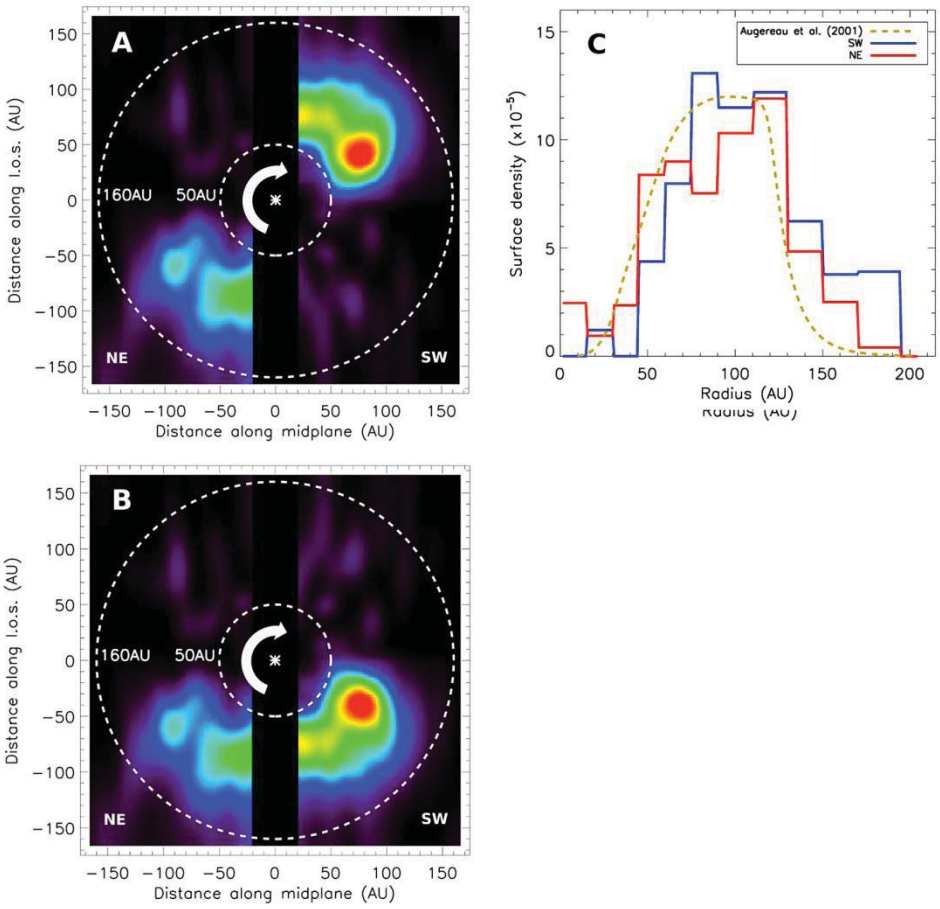

Fig. 3. Deprojected distributions of gas and dust around β Pic (*8*). (**A** and **B**) Two possible face-on distributions of the CO assuming circular orbital motion. (A) The two-clump distribution, interpreted as mean-motion resonances with an inner planet. In this case the bright southwest resonance lies on the far side of the star and is approaching us. (B) Single clump distribution, interpreted as a collision of ~Mars-mass objects; in this case the southwest clump is stationary and the "tail" of CO points in the direction of rotation. (**C**) Radial distribution of mm-sized dust in the southwest and northeast sectors of the disk, obtained by fitting consecutive annuli to the continuum distribution on the two sides (*12*). The dashed line is an axisymmetric model for the parent body distribution predicted from scattered light images of the sub-micron grains (*24*). Surface density units are cross-section area per unit disk area, in AU^2/AU^2.